Integrated analysis of high-throughput sequencing reveals the regulatory potential of hsa_circ_0035431 in HNSCC

XIAOYAN LIU[1,2*], LILI ZENG[1-3*], WENLONG WANG[1*], ZHIPENG LI[4], SIYUAN ZHOU[1,2], FANG WANG[1], YUE WANG[5], JING DU[3] and XIANGRUI MA[1]

[1]Department of Oral and Maxillofacial Surgery, Binzhou Medical University Hospital, Binzhou, Shandong 256600; [2]School of Stomatology, Binzhou Medical University, Yantai, Shandong 264000; [3]Medical Research Center, Binzhou Medical University Hospital, Binzhou, Shandong 256600; [4]Department of Stomatology, Jiaxing Hospital of Traditional Chinese Medicine, Jiaxing, Zhejiang 314001; [5]Department of Stomatology, Zibo Central Hospital, Zibo, Shandong 255000, P.R. China

Received April 1, 2023; Accepted July 14, 2023

DOI: 10.3892/ol.2023.14022

Abstract. Circular RNAs (circRNAs) are molecular sponges that are involved in regulation of multiple types of cancer. The present study aimed to screen and explore the key circRNA/microRNA (miRNA or miR)/mRNA interactions in head and neck squamous cell carcinoma (HNSCC) using bioinformatics. A total of six pairs of cancerous and adjacent healthy tissue were obtained from patients with HNSCC and genome-wide transcriptional sequencing was performed. Gene Ontology and Kyoto Encyclopedia of Genes and Genomes pathway enrichment analyses were performed on differentially expressed genes (DEGs). Moreover, expression levels of DEGs were verified in HNSCC cells and tissues using reverse transcription-quantitative (RT-q)PCR. A molecular regulatory network consisting of three circRNAs, seven miRNAs and seven mRNAs was constructed, resulting in identification of two signaling axes, hsa_circ_0035431/hsa-miR-940/fucosyltransferase 6 (FUT6) and hsa_circ_0035431/hsa-miR-940/cingulin-like 1 (CGNL1). FUT6 and CGNL1 were downregulated in HNSCC compared with adjacent healthy tissue and the expression levels of these genes were associated with tumor stage. Low FUT6 and CGNL1 expression levels were associated with lower overall survival rate and progression-free intervals in HNSCC. RT-qPCR demonstrated that hsa_circ_0035431, FUT6 and CGNL1 were downregulated in HNSCC cells and tissue and hsa-miR-940 was upregulated. Notably, these results were consistent with those obtained using high-throughput sequencing. In conclusion, hsa_circ_0035431 may participate in regulation of FUT6 and CGNL1 expression by sponging hsa-miR-940, thus, impacting the occurrence, development and prognosis of HNSCC.

Correspondence to: Dr Jing Du, Medical Research Center, Binzhou Medical University Hospital, 661 Huanghe Second Road, Binzhou, Shandong 256600, P.R. China
E-mail: djedith@126.com

Dr Xiangrui Ma, Department of Oral and Maxillofacial Surgery, Binzhou Medical University Hospital, 661 Huanghe Second Road, Binzhou, Shandong 256600, P.R. China
E-mail: 413865849@qq.com

*Contributed equally

Key words: cingulin-like 1, fucosyltransferase 6, head and neck squamous cell carcinoma, hsa_circ_0035431, hsa-miR-940

Introduction

Head and neck squamous cell carcinoma (HNSCC) is a common malignancy with ~600,000 cases new each year worldwide. Despite advances in screening, diagnosis and multimodal therapy, the 5-year survival rate for HNSCC is ~50% and is mainly associated with locally advanced progression and disease screening (1). Traditional clinicopathological parameters, such as tumor size, vascular infiltration and tumor node metastasis stage, do not aid in prediction of individual outcomes or determining risk stratification (2). Therefore, identification of novel potential biomarkers is required for predicting the occurrence and progression of locally advanced HNSCC.

MicroRNAs (miRNAs or miRs) are involved in the post-transcriptional regulation of gene expression via complete or partial base pairing with the 3'untranslated region of target genes (3). Circular RNAs (circRNAs) are closed, long, non-coding RNAs that are formed via direct reverse splicing of precursor mRNA that function by regulating RNA transcription and protein production, as well as sponging miRNAs (4). Notably, previous studies revealed that circRNAs participate in cancer pathogenesis by sponging miRNAs that target mRNA and circRNAs exhibit potential as predictive biomarkers and therapeutic targets for cancer treatment (5,6). In addition, a previous study demonstrated that circRNA/miRNA/mRNA networks are involved in the development and progression of multiple types of malignancy (7). Results of a meta-analysis demonstrated that nine circRNAs may serve as potential prognostic markers for HNSCC and these are associated with lower overall survival (OS) and poor clinicopathological outcomes in patients with HNSCC (8).

circRNAs are involved in the pathogenesis and progression of HNSCC through multiple mechanisms. For example, circCORO1C promotes laryngeal squamous cell carcinoma progression by modulating the let-7c-5p/PBX3 axis (9). Thus, further investigations into the specific molecular mechanisms underlying circRNA/miRNA/mRNA regulation are required to aid discovery of effective therapeutic targets.

With the development of next-generation sequencing (NGS), research has focused on comprehensive genomic analysis based on tumor molecular features, such as somatic mutations and copy number variation. Exploring the interactions between various RNAs may provide novel insights into the initiation and progression of HNSCC. Thus, the present study performed NGS on six pairs of HNSCC cancer and adjacent healthy tissues to detect RNAs with high levels of differential expression. Potential interactions between circRNAs/miRNAs/mRNAs were predicted using bioinformatics and online databases. The present study aimed to provide a novel theoretical basis for understanding the molecular regulatory role of circRNAs in HNSCC.

Materials and methods

Patient information and sample acquisition. In total, six pairs of HNSCC and adjacent healthy tissue were obtained from patients (4 male and 2 female patients, aged 40-82 years) admitted to The Binzhou Medical University Hospital (Binzhou, China) and The West China Hospital of Stomatology, Sichuan University (Sichuan, China) between December 2020 and January 2021. The adjacent tissues were selected at ~5 mm from the edge of the lesion tissue, and their size was 3-5 mm. Notably, patients had not received preoperative chemotherapy or radiotherapy. All samples were obtained during surgery and immediately stored in liquid nitrogen and were confirmed to be HNSCC following histopathological examination. Written informed consent was obtained from patients and relatives of patients >18 years of age, where required.

Inclusion criteria were as follows: i) Primary sites: Cheek, tongue, lip, gum, floor of mouth, tongue and tonsil parapharyngeal; ii) patients diagnosed with SCC by routine pathology after surgery in the Department of Pathology, Affiliated Hospital of Binzhou Medical College; iii) patients who underwent the first operation without radiotherapy and/or chemotherapy before surgery; iv) patients with preoperative clinical stages of T3 and T4; and v) patient's with informed consent. Exclusion criteria were as follows: i) Patients with recurrence and metastasis who were re-admitted for surgery; ii) patients who had received surgical treatment in other hospitals and were re-admitted to Affiliated Hospital of Binzhou Medical College for surgical treatment.

Whole-genome sequencing analysis. Firstly, ribosomal RNA was removed from the total RNA, and then RNase R enzyme was used to break the RNA into short fragments of 250-300 bp. The first strand of cDNA was synthesized using the fragmented RNA as the template and random oligonucleotides as the primer, and then RNase H was used to degrade the RNA strand. The second strand of cDNA was synthesized by dNTPs (dUTP, dATP, dGTP and dCTP) in the system of DNA polymerase I. The purified double-stranded cDNA was end-repaired, A-tailed and connected to sequencing joints, and 350-400 bp cDNA was screened using AMPure XP beads (no. AG21101; Accurate Biotechnology Co., Ltd.; Hunan Aikerui Bioengineering Co., Ltd.). The second strand of cDNA containing U was degraded by USER enzyme, and the library was obtained by PCR amplification (ABI2720; Applied Biosystems; USA). The extraction method used was a TRNzol Universal Reagent+small column (cat. no. DP424+RK177-A). The kit was a NEB Next® Multiplex Small RNA Library Prep Set for Illumina® (cat. no. NEB E7300L). The sequencing instrument platform was an Illumina Novaseq 6000 (Illumina, Inc.) and the sequencing strategy was SE50. The sequencing of smallRNA in the current project was conducted from the 5'-3' direction (forward, 5'-GTTCAGAGTTCTACA GTCCGACGATC-3' and reverse, 5'-AGATCGGAAGAGCAC ACGTCT-3'). The reagents used for PCR were all contained in the NEB Next® Multiplex Small RNA Library Prep Set for Illumina. A chain-specific library has many advantages, such as the same amount of data can obtain more effective information; more accurate gene quantification, localization and annotation information can be obtained. An Agilent 2100 bioanalyzer (Agilent Technologies, Inc.) was used to detect the insert size of the library, and the insert size was about 250-300 bp, which was in line with the expectation. The effective concentration of the library was >2 nM, which ensured the quality of the sample library. NGS was used to detect differentially expressed circRNAs, miRNAs and mRNAs in HNSCC and adjacent healthy tissues. Sample detection, library construction and testing and computer sequencing were completed by Beijing Novogene Technology Co., Ltd. Briefly, a strand-specific library was constructed by removing ribosomal RNA. Following library inspection, Illumina PE150 sequencing was performed in accordance with effective centralization and data output requirements. RNA sequencing (RNAseq) data were compared and analyzed using Tophat2 (version 2.0.8) (10) software. edgeR (version 4.2.2) (11) was used for analysis of differentially expressed RNAs; differentially expressed circRNAs, miRNAs and mRNAs were screened based on $P<0.05$ and $|\log2FC|>1$. Hierarchical clustering was performed based on all differentially expressed transcripts to construct expression profiles. The expression values of all samples were clustered and visualized in heat maps using hierarchical clustering. The mainstream hierarchical clustering method was used to convert log10 (FPKM+1) values and cluster them.

Gene Ontology (GO) and Kyoto Encyclopedia of Genes and Genomes (KEGG) analysis. To explore the biological pathways of potential target genes, GOseq (http://www.geneontology.org/) (12) and KEGG Orthology Based Annotation System (version 2.0) (13) software were used to perform GO and KEGG pathway enrichment analysis of target genes. GO is a comprehensive database describing gene function, which is divided into molecular function (MF), biological process (BP) and cellular component (CC). The results are presented as bar graphs and bubble plots.

circRNA/miRNA/mRNA network construction. miRNAs associated with the development and prognosis of HNSCC were screened using OncomiR (oncomir.org). MiRanda

(v3.3a) (14) software was used for predicting the top five differentially expressed circRNA-targeted miRNAs. MiRanda and RNAhybrid (v2.1) (15) were used for target gene prediction of key miRNAs. Venn analysis was further performed through the R-VennDiagram package (ggplot2, version3.3.6; VennDiagram, version 1.7.3).

Visualization of miRNA intersection results. mRNAs associated with HNSCC prognosis were downloaded from Gene Expression Profiling Interactive Analysis (GEPIA; gepia.cancer-pku.cn/) for analysis. circRNA/miRNA and miRNA/mRNA pairs were merged and Cytoscape (version 3.5.1) (https://cytoscape.org/) was used to visualize the topological network of circRNA/miRNA/mRNA.

Targeted binding strength analysis. mRNA and miRNA sequences were downloaded from National Center for Biotechnology Information (NCBI; ncbi.nlm.nih.gov/) and miRbase (mirbase.org/index.shtml), respectively. NCBI Blast (blast.ncbi.nlm.nih.gov/Blast.cgi) was used to compare sequences of hsa_ circ_0035431 and hsa_circ_0035432 to screen out key circRNAs with potential roles in HNSCC. The binding sequence and strength of miRNA/mRNA was analyzed using R22 (version 2; cm.jefferson.edu/rna22/).

Comprehensive analysis of online databases and The Cancer Genome Atlas (TCGA). GEPIA (gepia.cancer-pku.cn/) and UALCAN (ualcan.path.uab.edu/) were used to compare transcription levels of FUT6 and CGNL1 in HNSCC tissue and healthy samples, with further analysis by subtypes and stages. Patients with complete expression data of FUT6 and CGNL1 were screened using TCGA (portal.gdc.cancer.gov/) database. Pair expression (ggplot2, version 3.3.6; stats, version 4.2.1; car, version 3.1-0), logistic regression (astats, version 4.2.1) and prognosis analysis (survival, version 3.3.1; survminer, ggplot2, version 3.3.6) of FUT6 and CGNL1 in healthy and tumor tissue was performed using R software (version 4.2.1; R Core Team) and associated R packages to evaluate association with clinical variables and patient survival.

Cell culture. Oral squamous Hok and oral squamous cell carcinoma SCC25 and HSC2 cell lines were purchased from the American Type Culture Collection and stored in liquid nitrogen (-196˚C) in the Medical Research Center, Binzhou Medical University Hospital. All cell lines were cultured in DMEM (VivaCell Biotechnology GmbH) supplemented with 10% fetal bovine serum (HyClone; Cytiva) and 1% penicillin/streptomycin (100 mg/ml; VivaCell Biotechnology GmbH) at 37˚C in 5% CO_2.

RNA extraction and reverse transcription-quantitative (RT-q)PCR. Total RNA was extracted from all tissue and cell samples using AG RNA ex Pro Reagent (Accurate Biotechnology Co., Ltd.; Hunan Aikerui Bioengineering Co., Ltd.) Total RNA was reverse-transcribed into cDNA using an Evo M-MLV RT kit with gDNA Clean for qPCR II (Accurate Biotechnology Co., Ltd.). The reverse transcription reaction conditions were as follows: i) 42˚C for 2 min; store at 4˚C; ii) 37˚C for 15 min; 85˚C for 5 sec; store at 4˚C. hsa-miR-940 was reverse-transcribed using miRNA 1st Strand cDNA Synthesis kit (Accurate Biotechnology Co., Ltd.). The reverse transcription reaction condition was 37˚C for 60 min, 85˚C for 5 min and storage at 4˚C. qPCR was performed using a SYBR® Green Premix Pro Taq HS qPCR kit (Accurate Biotechnology Co., Ltd.). The following thermocycling conditions were used: 40 cycles of 95˚C for 30 sec, 95˚C for 5 sec and 60˚C for 30 sec. RT-qPCR data were collected using the CFX96 Real-Time PCR Detection System (Bio-Rad Laboratories, Inc.) and expression levels were quantified using the $2^{-\Delta\Delta Cq}$ method (16). β-actin and U6 were used as internal controls for mRNA and miRNA, respectively. All primers were designed by Accurate Biotechnology Co., Ltd. (Table I).

Table I. Sequences of primers for reverse transcription-quantitative PCR.

Gene	Primer sequence (5'-3')
FUT6	F: GACGATCCCACTGTGTACCCTA
	R: TGTTAAAAGGCCACGTCCACAG
CGNL1	F: GCAGATGGAGGACAAGGTGTCT
	R: CTCGCAGCTCTCTCCTGAAGT
hsa-miR-940	F: AGGGCCCCCGCTCCCCAA
circRNA_	F: GGAAATAACCAACTGGAACAGTGA
0035431	R: TAGGAGCCTGCCTTGGAGTTC
β-actin	F: TGGCACCCAGCACAATGAA
	R: CTAAGTCATAGTCCGCCTAGAAGCA
U6	F: CTCGCTTCGGCAGCACA
	R: AACGCTTCACGAATTTGCGT

FUT6, fucosyltransferase 6; CGNL1: cingulin-like 1; F, forward; R, reverse; miR, microRNA; circ, circular.

Statistical analysis. RT-qPCR data were analyzed by Graph-pad Prism 8.0 software (Graphpad Inc.; Dotmatics). Three independent replicate experiments were performed, and data are presented as the mean ± SD. The tissue samples were statistically analyzed by paired Student's t-test. One-way ANOVA with Dunnett's post hoc test was used for comparison of cell samples. $P<0.05$ was considered to indicate a statistically significant difference.

Results

Screening of differentially expressed RNA. Whole-genome transcriptional sequencing identified 6,750 circRNAs, 265 miRNAs and 19,816 mRNAs. In total, 169 circRNAs, 214 miRNAs and 1,270 mRNAs were differentially expressed. Volcano plots were used to illustrate differential expression (Fig. 1A-C). The expression patterns of circRNAs, miRNAs and mRNAs were distinguished using hierarchical clustering analysis. circRNA, miRNA and mRNA expression patterns in HNSCC differed from those in adjacent healthy tissues (Fig. 1D-F).

GO and KEGG analysis. Functions of the majority of circRNAs are yet to be annotated and functional prediction of circRNAs is largely based on the annotation of the

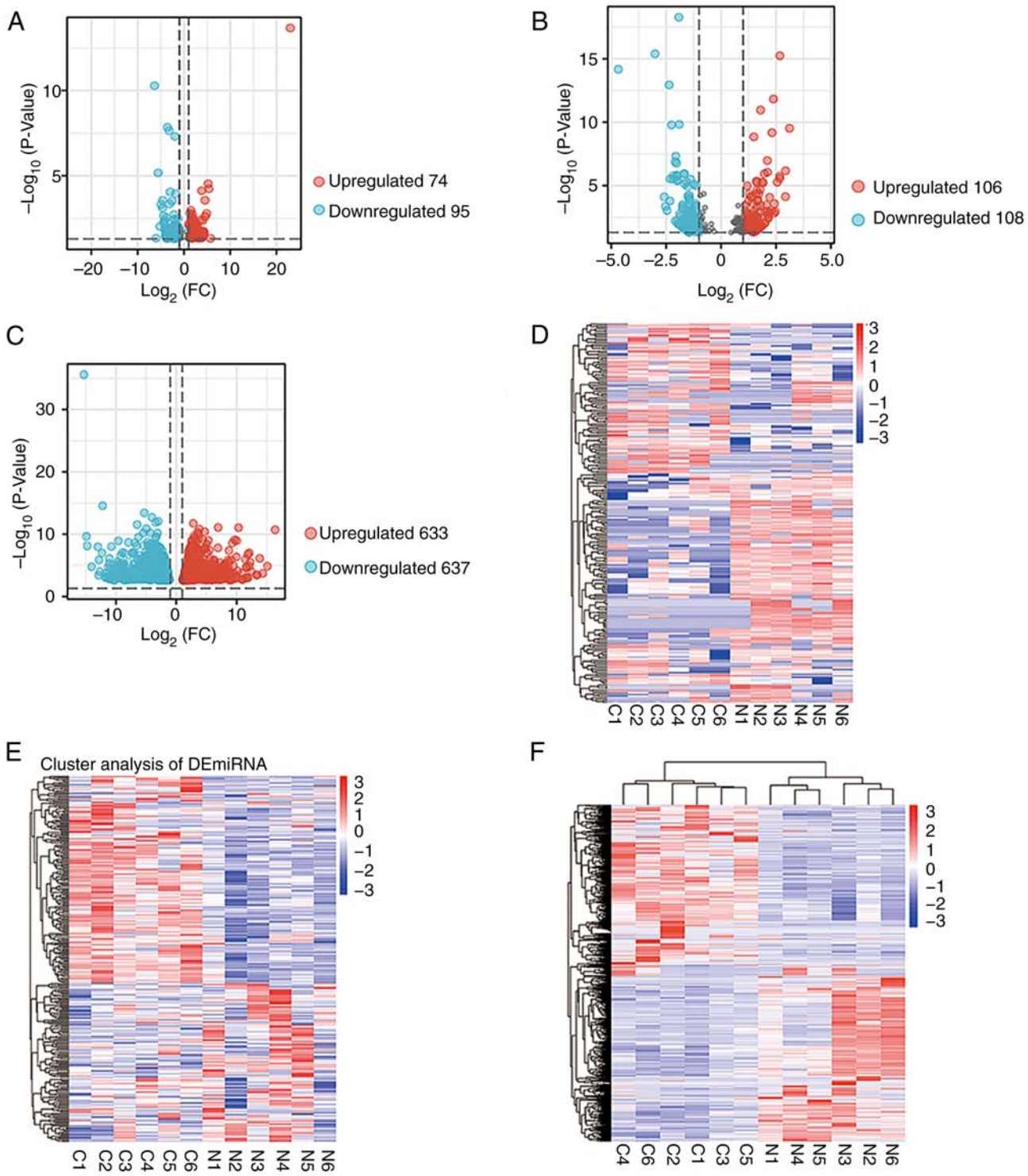

Figure 1. Identification of DE RNAs of HNSCC. Volcano plots of (A) DECs, (B) DEmiRNAs and (C) DEGs in HNSCC. Gray dots indicate no significant difference. P<0.05, |log2FC|>1. Heatmap of (D) DECs, (E) DEmiRNAs and (F) DEGs in HNSCC. HNSCC, head and neck squamous cell carcinoma; DE, differentially expressed; C, circular RNA; miRNA, microRNA; G, gene.

protein codes they interact with. As such, GO and KEGG analysis of dysregulated mRNAs may predict the function of circRNAs (17). GO analysis in the present study demonstrated that DEGs were primarily enriched in BP terms such as 'extracellular structure organization' (GO:0043062), 'extracellular matrix organization' (GO:0030198) and 'type 1 interferon signaling pathway' (GO: 0060337). The most abundant CC terms included 'collagen-containing extracellular matrix' (GO:0062023), 'collagen trimer' (GO:0005581) and 'extracellular matrix component' (GO:0044420). The most enriched MFs included 'extracellular matrix structural constituent' (GO:0005201), 'extracellular matrix structural constituent conferring tensile strength' (GO:0030020) and 'glycosaminoglycan binding' (GO:0005539). The eight most significantly enriched GO terms for up- and downregulated mRNAs in BP, CC and MF categories are displayed in Fig. 2.

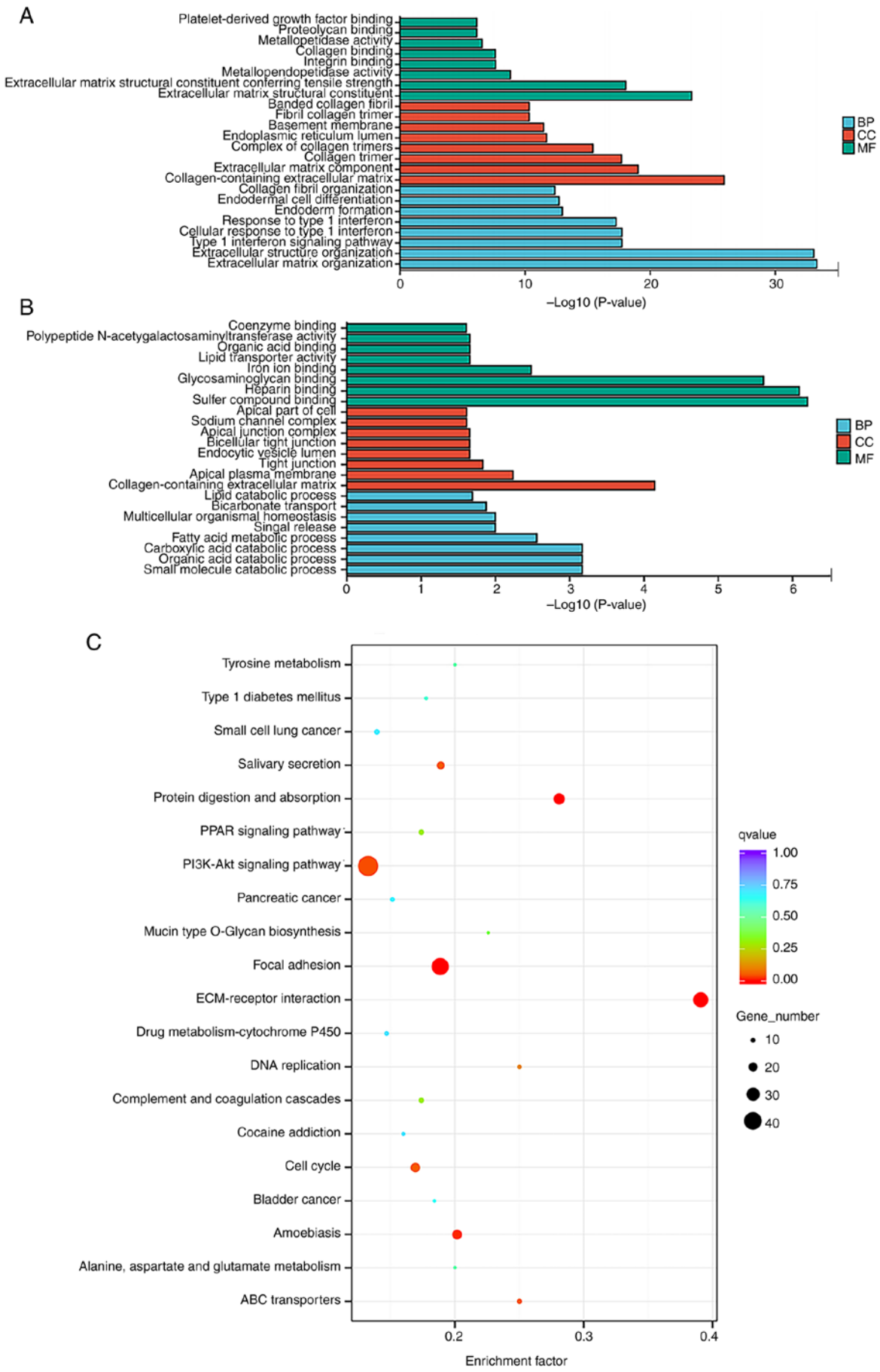

Figure 2. GO and KEGG analyses. GO annotation of (A) up- and (B) downregulated mRNAs. (C) KEGG pathway enrichment analysis of dysregulated mRNAs. Q-value indicates degree of enrichment. GO, Gene Ontology; KEGG, Kyoto Encyclopedia of Genes and Genomes; BP, biological process; CC, cellular component; MF, molecular function.

Table II. Top five differentially expressed circRNAs.

circRNA	Regulation	log2FC	P.adj	Chromosome	Gene type	Source gene
hsa_circ_0035432	Down	-6.0217	0.045209	15	Exonic	CGNL1
hsa_circ_0035431	Down	-5.5869	$6.65x10^{-6}$	15	Exonic	CGNL1
novel_circ_0010113	Down	-6.3637	$5.20x10^{-11}$	6	Exonic	RIMS1
hsa_circ_0001860	Up	5.7202	0.046254	9	Exonic	ZCCHC7
novel_circ_0009946	Up	22.9550	$2.15x10^{-14}$	6	Intergenic	NA

circ, circular; CGNL1, cingulin-like 1; RIMS1, regulating synaptic membrane exocytosis 1; ZCCHC7, zinc finger CCHC-type containing 7; NA, not applicable.

KEGG pathway analysis identified 263 pathways associated with dysregulated mRNAs, which were primarily enriched in the 'PI3K-Akt signaling pathway', 'focal adhesion' and 'ECM-receptor interaction pathways', demonstrating the key role of these factors in HNSCC. The top 20 most enriched pathways for protein-coding gene dysregulation are listed in Fig. 2.

Construction of the circRNA/miRNA/mRNA network. The target genes of the top five differentially expressed circRNAs were identified using miRanda (Table II) and the results demonstrated 714 target-binding miRNAs. Oncomir database predicted 468 miRNAs associated with the progression and prognosis of HNSCC. Differentially expressed miRNAs were overlapped with results of the databases to obtain 30 key miRNAs (Fig. 3A). The target gene prediction of 30 miRNAs using miRanda and RNA hybridization were overlapped with DEGs to obtain 334 mRNAs (Fig. 3B), constructing a network including five circRNAs, 30 miRNAs and 334 mRNAs (Fig. 4A). In total, 500 mRNAs associated with HNSCC prognosis were predicted using GEPIA, overlapping with the aforementioned 334 overlapped mRNAs, yielding seven key mRNAs (Fig. 3C). Thus, a network of three circRNAs, seven miRNAs and seven mRNAs was constructed (Fig. 4B). In total, eight regulatory axes were determined based on intermolecular regulatory interactions (Table III).

miRNA/mRNA target binding sequence and intensity analysis. miRNA and mRNA binding regions were determined and intensity analysis was performed using R22 (Table IV). Compared with that in ECHDC2 and EGF, miRNA and mRNA intensity analysis demonstrated increased binding of hsa-miR-940 to FUT6 and CGNL1, leading to the identification of four regulatory axes (Table V). hsa_circ_0035431 and hsa_circ_0035432 sequences were compared using NCBI and demonstrated a complete overlap of 1,818 base pairs, with the sequence of hsa_circ_0035431 being more closely aligned. Therefore, hsa_circ_0035431/hsa-miR-940/FUT6 and hsa_circ_0035431/hsa-miR-940/CGNL1 were selected for further analysis.

Expression of FUT6/CGNL1 in HNSCC. Transcription levels of FUT6 and CGNL1 in HNSCC were investigated using the GEPIA2 online database. FUT6 and CGNL1 mRNA expression levels were significantly decreased in HNSCC compared with healthy tissue (Fig. 5A and C). Paired sample analysis using data obtained from TCGA confirmed the aforementioned findings (Fig. 5B and D).

Table III. circRNA/miR/mRNA regulatory axes.

circRNA	miR	mRNA
hsa_circ_0035431	hsa-miR-3176	ECHDC2
hsa_circ_0035432	hsa-miR-3176	ECHDC2
hsa_circ_0035431	hsa-miR-940	FUT6
hsa_circ_0035432	hsa-miR-940	FUT6
hsa_circ_0035431	hsa-miR-940	CGNL1
hsa_circ_0035432	hsa-miR-940	CGNL1
novel_circ_0010113	hsa-miR-93-3p	EGF

circ, circular; miR, microRNA; ECHDC2, enoyl coenzyme A hydratase-containing domain 2; FUT6, fucosyltransferase 6; CGNL1, cingulin-like 1; EGF, epidermal growth factor.

Association of FUT6 and CGNL1 expression with clinical characteristics and survival. The subgroup analysis of pathological characteristics of HNSCC samples using UALCAN database demonstrated a decrease in FUT6 and CGNL1 transcription levels. Subgroup analysis of sex, age, disease stage and lymph node metastasis demonstrated that expression levels of FUT6 and CGNL were significantly lower in patients with HNSCC compared with controls (Figs. 6 and 7). Logistic regression analysis of TCGA data indicated that FUT6 expression was lower in T3 and T4 than in T1 and in stages II and IV than at stage I. Expression of CGNL1 was lower in T3 and T4 than in T1 (Table VI). In addition, increased FUT6 and CGNL1 expression was independent of sex, age and lymph node and distant metastasis (Tables VI and VII). To analyze clinical significance of FUT6 and CGNL1, prognostic analysis was performed using TCGA. Increased FUT6 and CGNL1 expression was associated with longer OS and progression-free interval (PFI) of patients with HNSCC (Fig. 8).

Validation of differential expression of hsa_circ_0035431, hsa-miR-940, FUT6 and CGNL1 in HNSCC. RT-qPCR was performed using the same RNA samples used in sequencing analysis. Results demonstrated that the expression levels of hsa_circ_0035431, FUT6 and CGNL1 were decreased and

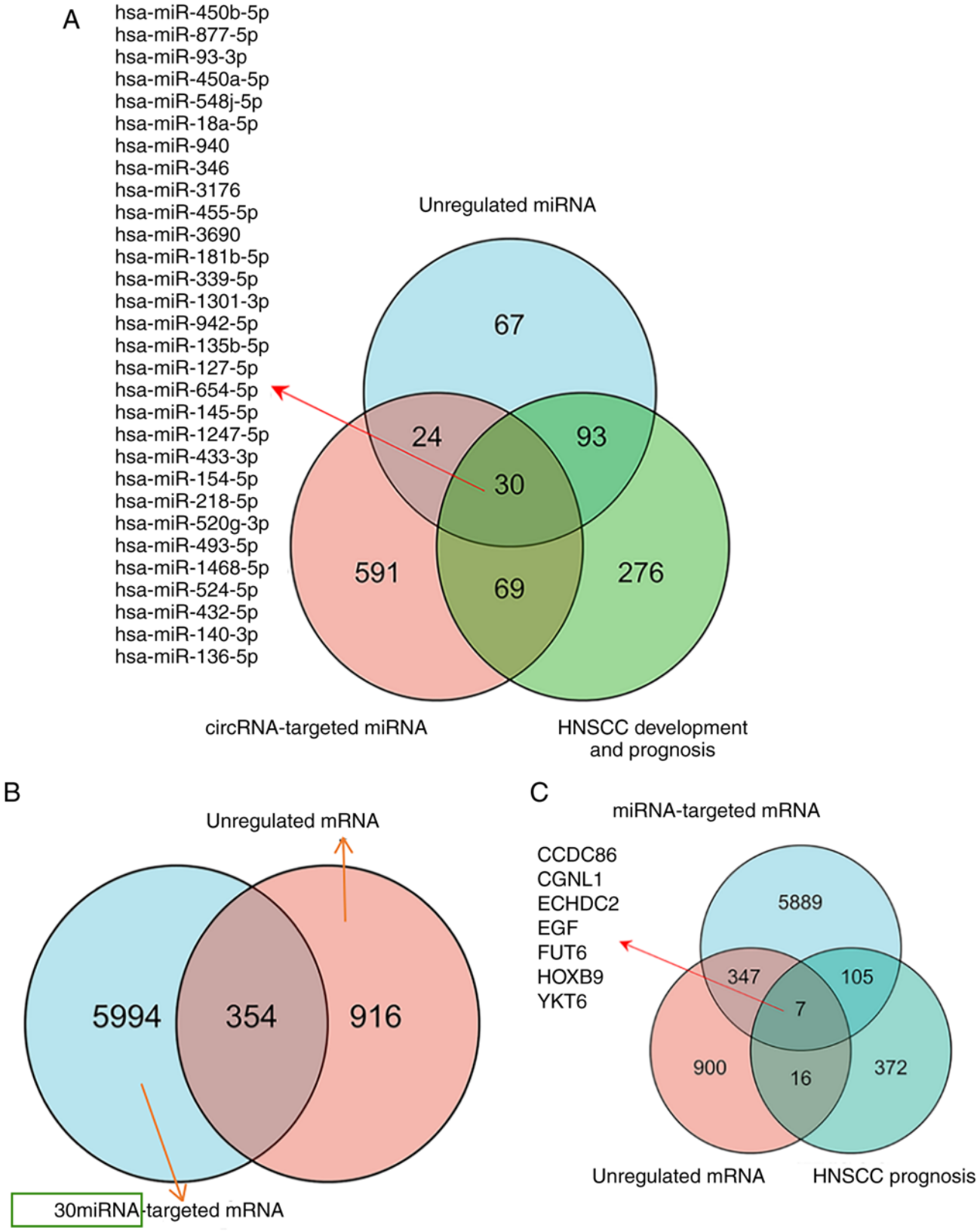

Figure 3. Identification of target miRNA and mRNA. Identification of (A) 30 miRNAs, (B) 334 mRNAs and (C) seven target mRNAs by Venn analysis. miRNA, microRNA; HNSCC, head and neck squamous cell carcinoma; circ, circular.

hsa-miR-940 expression levels were elevated in HNSCC compared with the HOK and adjacent groups (Fig. 9A-D). Notably, these results were consistent with those obtained using transcriptome sequencing (Fig. 9E-H).

Discussion

HNSCC is the seventh most common type of cancer in the world; however, treatment is complex and options include

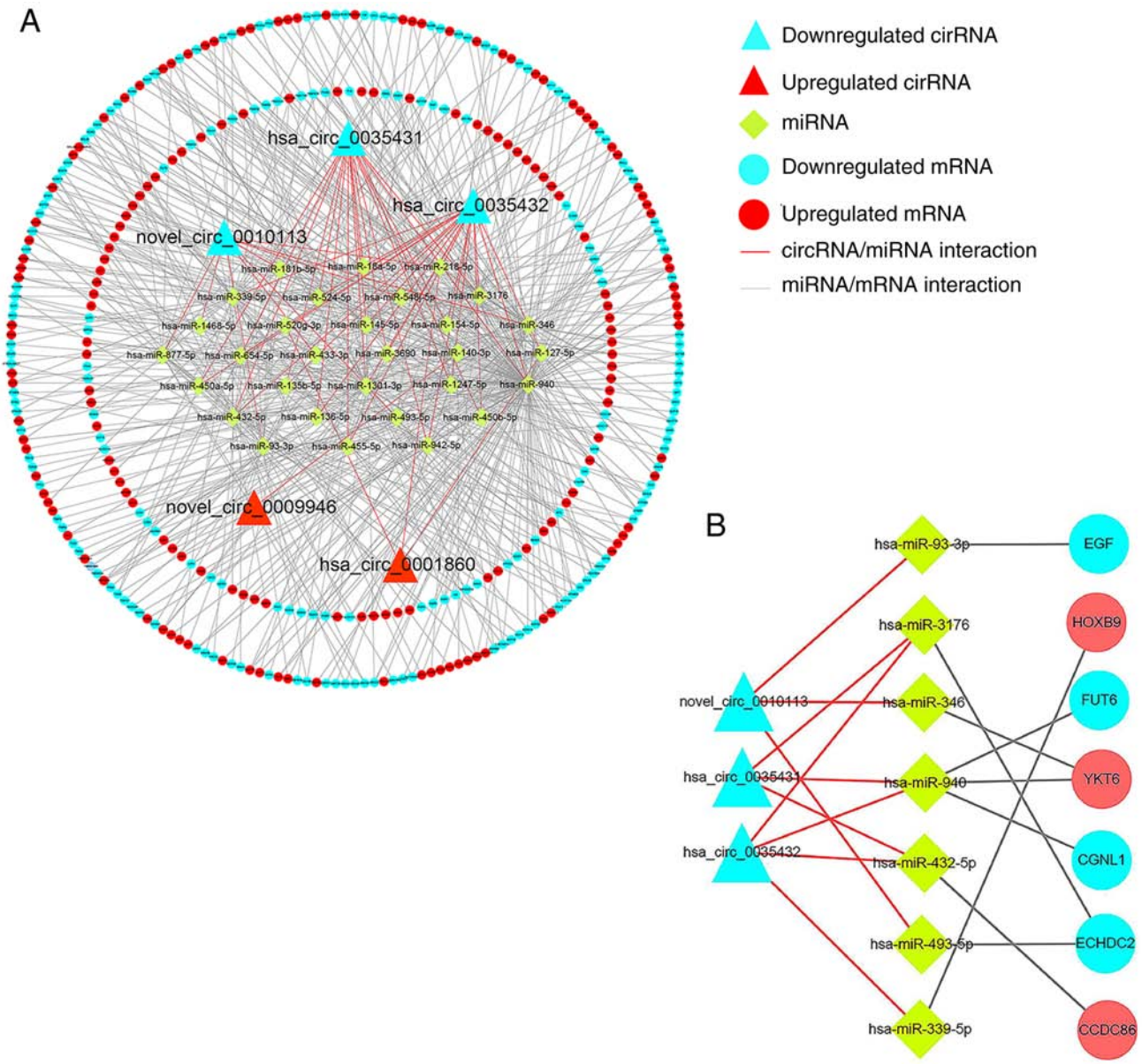

Figure 4. Construction of circRNA/miRNA/mRNA network. Networks of (A) five circRNAs, 30 miRNAs and 354 mRNAs and (B) three circRNAs, seven miRNAs and seven mRNAs. circ, circular; miRNA, microRNA.

surgery, radiotherapy and chemotherapy (1). Determining the underlying pathogenic mechanisms may aid discovery of effective treatment options to improve the survival rate of patients.

A total of 1-2% of transcribed genes encode proteins in eukaryotic cells and the majority of remaining genes are transcribed into non-coding RNAs (ncRNAs) (18). ncRNAs are divided according to their length as small (18-200 nucleotides) and long ncRNAs (>200 nucleotides). miRNAs are the most commonly studied type of ncRNA (19,20). circRNAs, another type of ncRNA with an average length of 1 kb, serve key roles in tumors through acting as molecular sponges for miRNAs (21). Although circRNAs were discovered in eukaryotes as early as 1991, the circRNA transcriptome has only been studied in detail in recent years (22). A previous study demonstrated that circRNAs serve as endogenous competitive RNAs, thereby regulating proliferation, invasion and other physiological activities of tumor cells (23). High-throughput sequencing is widely used in circRNA studies to identify associated functions (24,25). BPs, MFs and signaling pathways may aid in determining the mechanisms of HNSCC onset and progression. Numerous circRNAs serve a regulatory role in colorectal cancer progression (26). Microtubule cross-linking factor 1 circRNA promotes progression of advanced laryngeal squamous carcinoma by inhibiting C1q-binding protein ubiquitin degradation and mediating β-catenin activation, demonstrating the pro-carcinogenic role of circRNA (27). circ_0109291 is highly expressed in cisplatin-resistant oral squamous cell carcinoma tissue and promotes cisplatin resistance by sponging miR-188-3p, suggesting the therapeutic efficacy of circRNA (28). Therefore, clarifying the regulatory role of RNAs in HNSCC may provide a novel theoretical basis for disease progression and treatment.

Table IV. miR and mRNA binding regions and intensity.

RNA	miR/mRNA binding site	Folding energy, kcal/mol	P-value
FUT6	5'-3': TGGGA-CCTGTGCCCAGCCTA	-18.50	$3.51x10^{-1}$
hsa-miR-940	3'-5': CCCCTCGCCCCCGGGACGGAA		
FUT6	5'-3': CTCCAGTGGTGAAGACCCAGCCTG	-15.30	$2.41x10^{-2a}$
hsa-miR-940	3'-5': CCCCTCGCC-C-CC-GGGACGGAA		
CGNL1	5'-3': CAGGAGCAGAAGCAGTTGTCTG	-15.80	$3.81x10^{-2a}$
hsa-miR-940	3'-5': CCCCTCGCCCCCG-GGACGGAA		
CGNL1	5'-3': CTGCAGCTATGGCCTTGTTTG	-16.80	$1.16x10^{-2a}$
hsa-miR-940	3'-5': CCCCTCGCCCCCGGGACGGAA		
CGNL1	5'-3': TCAGAGTGGTCAGCCCAGTTTA	-17.30	$2.73x10^{-1}$
hsa-miR-940	3'-5': CCCCTCGCC-CCCGGGACGGAA		
CGNL1	5'-3': GGGGTGATTCTCACCTCTGCCTG	-19.44	$2.76x10^{-2a}$
hsa-miR-940	3'-5': CCCCTC--GCCCCCGGGACGGAA		
CGNL1	5'-3': ATGGTTTGGTCGCTTTGGTTG	-12.60	$5.27x10^{-2}$
hsa-miR-940	3'-5': CCCCTCGCCCCCGGGACGGAA		
EGF	5'-3': ATGGAACTCTGCTCAGC-CAGCAGA	-20.30	$1.18x10^{-1}$
hsa-miR-93-3p	3'-5': GCCCTT--CACGA-TCGAGTCGTCA		
EGF	5'-3': TGAGGA-TGGCCAG-GCAGCAGA	-16.20	$9.61x10^{-2}$
hsa-miR-93-3p	3'-5': GC-CCTTCACGATCGAGTCGTCA		
ECHDC2	5'-3': AGTGAAGGGCGTGTTC-TGTGCAG	-15.50	$1.73x10^{-1}$
hsa-miR-493-5p	3'-5': TTACTTTCGG--ATGGTACATGTT		
ECHDC2	5'-3': CGGG-AGGACC-GGCAAGT	-13.80	$1.73x10^{-1}$
hsa-miR-3176	3'-5': GGCCATCAGGGTCCGGTCA		

[a]P<0.05. The underlined bases indicate the binding site between mRNA and miR. miR, microRNA; ECHDC2, enoyl coenzyme A hydratase-containing domain 2; FUT6, fucosyltransferase 6; CGNL1, cingulin-like 1; EGF, epidermal growth factor.

Table V. circRNA-miR-mRNA regulatory axes.

circRNA	miR	mRNA
hsa_circ_0035431	hsa-miR-940	FUT6
hsa_circ_0035432	hsa-miR-940	FUT6
hsa_circ_0035431	hsa-miR-940	CGNL1
hsa_circ_0035432	hsa-miR-940	CGNL1

miR, microRNA; circ, circular; FUT6, fucosyltransferase 6; CGNL1, cingulin-like 1.

circRNAs regulate gene expression through competitive binding to miRNA (29). miRNAs block protein translation and regulate mRNA stability at the post-transcriptional level by binding to miRNA recognition elements (30). circRNA/miRNA/mRNA interactions have been identified in progression and prognosis of non-small cell lung (31) and gastric cancer (32) and nasopharyngeal carcinoma (33). Although circRNA/miRNA/mRNA interactions serve a role in tumorigenesis and progression, the pathogenesis and potential treatment of HNSCC are poorly understood and further investigation is required.

In the present study, the whole genome of six pairs of HNSCC and adjacent healthy tissue were sequenced and the abnormal expression of circRNA, miRNA and mRNA were screened. In addition, key target genes, FUT6 and CGNL1 were determined by targeted prediction and online databases, yielding hsa_circ_0035431/hsa-miR-940/FUT6 and hsa_circ_0035431/hsa-miR-941/CGNL1 axes, which were associated with the occurrence, development and prognosis of HNSCC.

Results of a previous study demonstrated that hsa_circ_0035431 is the most differentially altered circRNA in patients with gastric cancer, suggesting that it may be involved in the pathological process of gastric cancer progression (34). However, the role of circRNA in HNSCC is yet to be fully elucidated. A previous study confirmed the role of miRNA-940 in tumor progression: miRNA-940 promotes gastric cancer cell proliferation and migration by regulating programmed death ligand 1 (35) and promotes invasion and metastasis through downregulation of zinc finger transcription factor 24 (36). Su *et al* (37) demonstrated that miR-940 overexpression promotes progression of human cervical cancer through inhibiting p27 and PTEN, highlighting that miRNA-940 inhibition may be a target for treatment of cervical cancer. In the present study, the Oncomir database and circRNA targeting prediction were

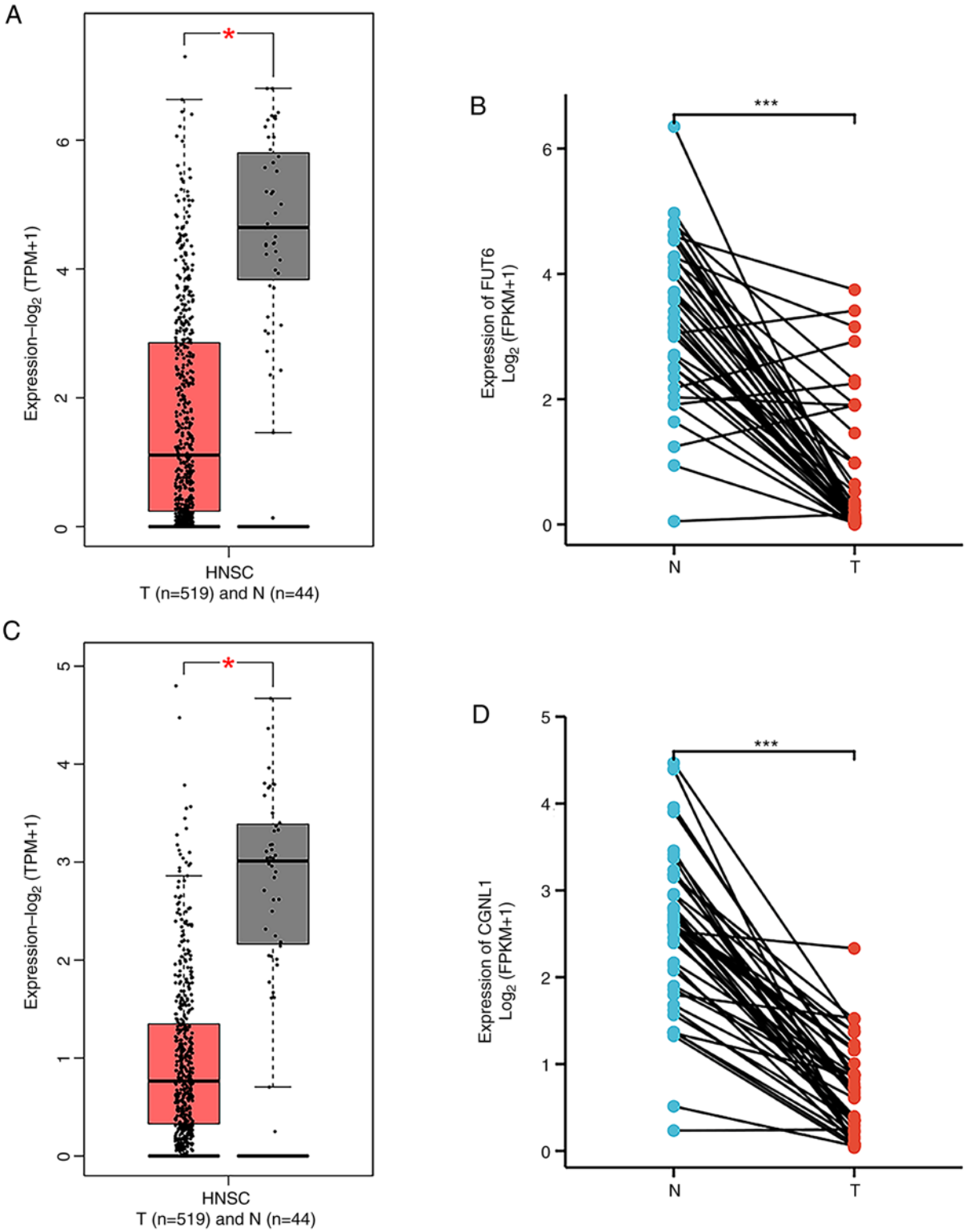

Figure 5. Expression of FUT6 and CGNL1. Expression of FUT6 in (A) GEPIA and (B) TCGA. Expression of CGNL1 in (C) GEPIA and (D) TCGA. *P<0.05 and ***P<0.001. FUT6, fucosyltransferase 6; CGNL1, cingulin-like 1; GEPIA, Gene Expression Profiling Interactive Analysis; TCGA, The Cancer Genome Atlas; T, tumor; N, normal; TPM, transcripts per million; FPKM, fragments per kilobase of transcript per million mapped reads.

used to determine whether hsa-miR-940 was associated with development and prognosis of HNSCC. An association between hsa_circ_0035431 and hsa-miR-940 was established, suggesting that the hsa_circ_0035431/hsa-miR-940 axis may be involved in progression and prognosis of HNSCC. In addition, the present study demonstrated FUT6 and CGNL1 were the target genes of hsa-miR-940 through target gene prediction.

FUT6 is a member of the FUT family and is involved in the synthesis of α-1,3-fucosyl bonds (38). A previous study demonstrated that high FUT6 expression is associated with lower event-free survival and OS; thus, FUT6

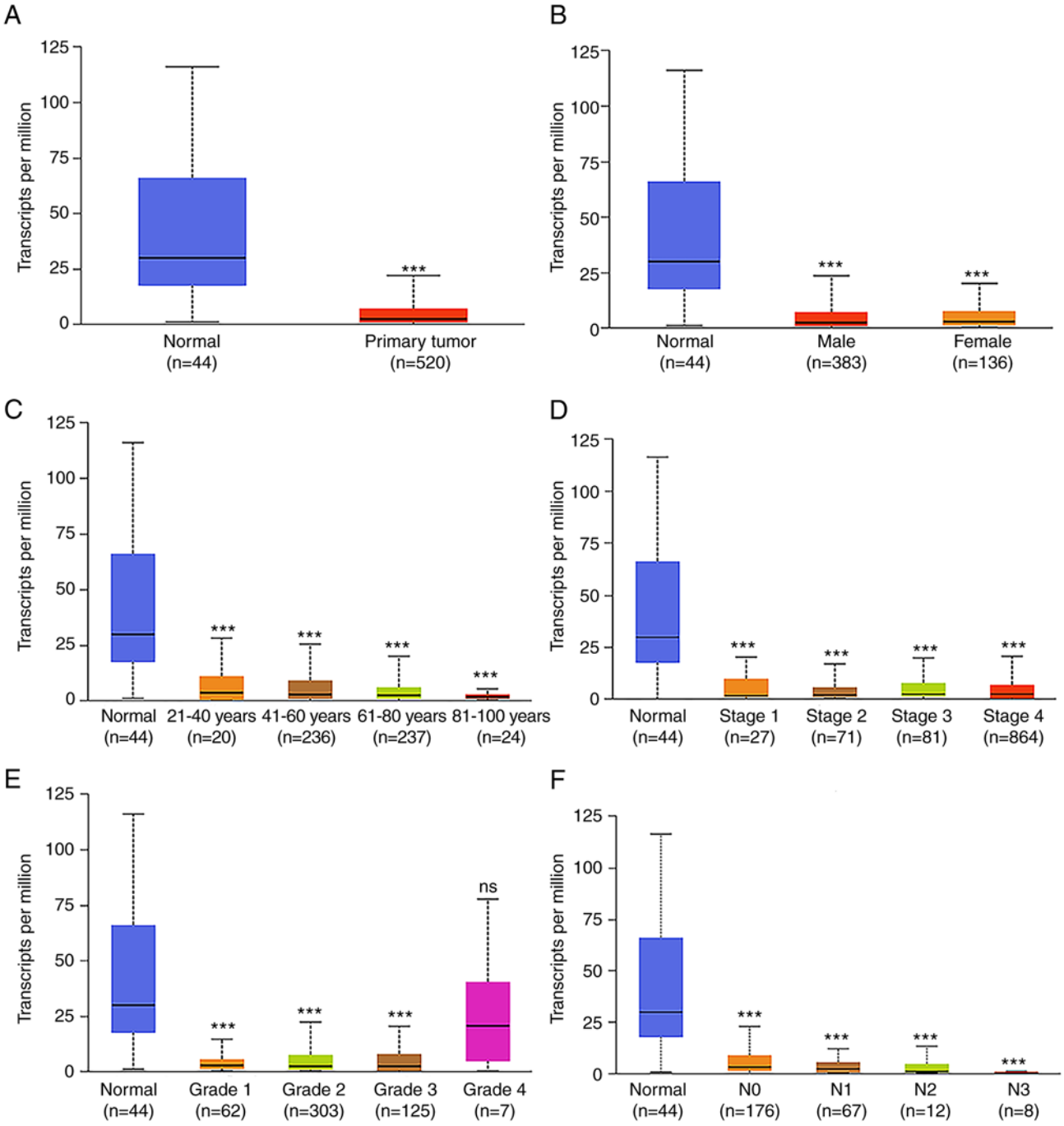

Figure 6. Transcription of FUT6 in patients with HNSCC. (A) Box-plot showing the relative expression of FUT6 in normal and HNSCC samples. Box-plot showing the relative expression of FUT6 in patients with HNSCC by (B) sex, (C) age, cancer (D) stage and (E) grade, and (F) nodal metastasis stage. Data were obtained from The Cancer Genome Atlas. ***P<0.001 vs. normal. FUT6, fucosyltransferase 6; HNSCC, head and neck squamous cell carcinoma; ns, not significant.

may serve as an independent adverse prognostic factor in patients with acute myeloid leukemia (39). Based on TCGA HNSCC cohort, Mai *et al* (40) revealed a robust differentially expressed metabolic enzyme-based prognostic signature, which included FUT6, for predicting clinical outcomes of HNSCC. Moreover, a novel 19-gene risk predictive score model, which included FUT6, was developed based on genes associated with lipid metabolism. The aforementioned study demonstrated that FUT6 may serve as a prognostic indicator and therapeutic target of gastric cancer (41). By contrast, Li *et al* (42) demonstrated that FUT6 overexpression may decrease the proliferation, migration and invasion of human breast cancer cells. Thus, it was hypothesized that FUT6 may be involved in different biological processes in numerous types of cancer.

CGNL1, also known as paracingulin, is an endothelial junctional complex protein localized to adhesion and tight junctions. CGNL1 serves important roles in regulating vascular growth in embryonic development and adult vascular-associated diseases (43). Low expression of CGNL1, the target gene of miR-149-3p, is associated with a poor prognosis in patients with uterine corpus endometrial carcinoma (44). Notably,

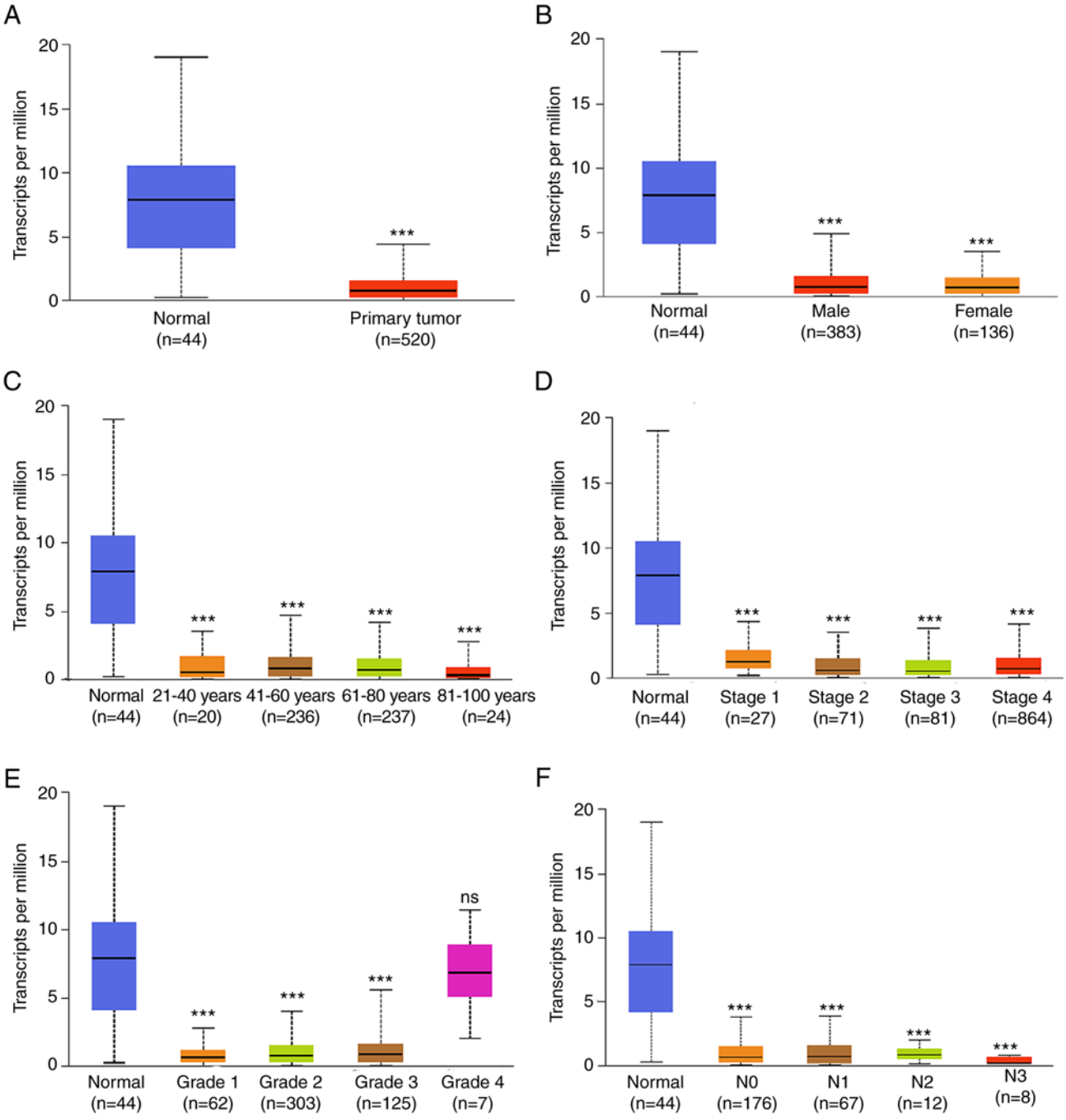

Figure 7. Transcription of CGNL1 in patients with HNSCC. (A) Box-plot showing the relative expression of CGNL1 in normal and HNSCC samples. Box-plot showing the relative expression of FUT6 in patients with HNSCC by (B) sex, (C) age, cancer (D) stage and (E) grade, and (F) nodal metastasis stage. Data were obtained from The Cancer Genome Atlas. ***P<0.001 vs. normal. CGNL1, cingulin-like 1; HNSCC, head and neck squamous cell carcinoma; ns, not significant.

CGNL1 may be involved in processes associated with progesterone resistance (45). Moreover, CGNL1 is a prognostic gene for carriers of the HNSCC TP53 mutation (46). A previous study indicated that CGNL1 may act as a urine biomarker of high-grade bladder urothelial carcinoma (HGBC), thus exhibiting potential as a diagnostic indicator, prognostic predictor and treatment target for HGBC. Thus, CGNL1 may improve prognosis of patients with HGBC (47).

Through data mining, the expression levels of FUT6 and CGNL1 were investigated in HNSCC in the present study. Results from the GEPIA database demonstrated that FUT6 and CGNL1 expression were lower in tumor tissues of patients with HNSCC compared with adjacent healthy tissue. Subsequently, the expression levels of FUT6 and CGNL1 were compared using UALCAN and TCGA databases. FUT6 and CGNL1 expression levels were associated with the staging of patients with HNSCC. In addition, patients with low FUT6 and CGNL1 expression levels exhibited decreased OS and PFI compared with the those with high expression levels. Collectively, the present study demonstrated that FUT6 and CGNL1 may serve key roles in the development and prognosis of HNSCC.

Table VI. Logistic regression analysis of fucosyltransferase 6.

Characteristic	n	Odds ratio (95% CI)	P-value
T2 vs. T1	177	0.543 (0.238-1.181)	0.132
T3 vs. T1	164	0.449 (0.196-0.983)	0.050[a]
T4 vs. T1	212	0.432 (0.192-0.927)	0.035[a]
N1 vs. N0	319	0.650 (0.386-1.083)	0.101
N2 vs. N0	393	1.054 (0.703-1.582)	0.798
N3 vs. N0	246	0.731 (0.142-3.385)	0.686
M1 vs. M0	477	0.672 (0.088-4.093)	0.665
Stage II vs. I	114	0.295 (0.090-0.840)	0.029[a]
Stage III vs. I	121	0.386 (0.118-1.092)	0.088
Stage IV vs. I	291	0.342 (0.108-0.920)	0.045[a]
Male vs. female	502	0.751 (0.504-1.117)	0.158
Age >60 vs. ≤60 years	501	0.873 (0.614-1.239)	0.447

[a]P<0.05

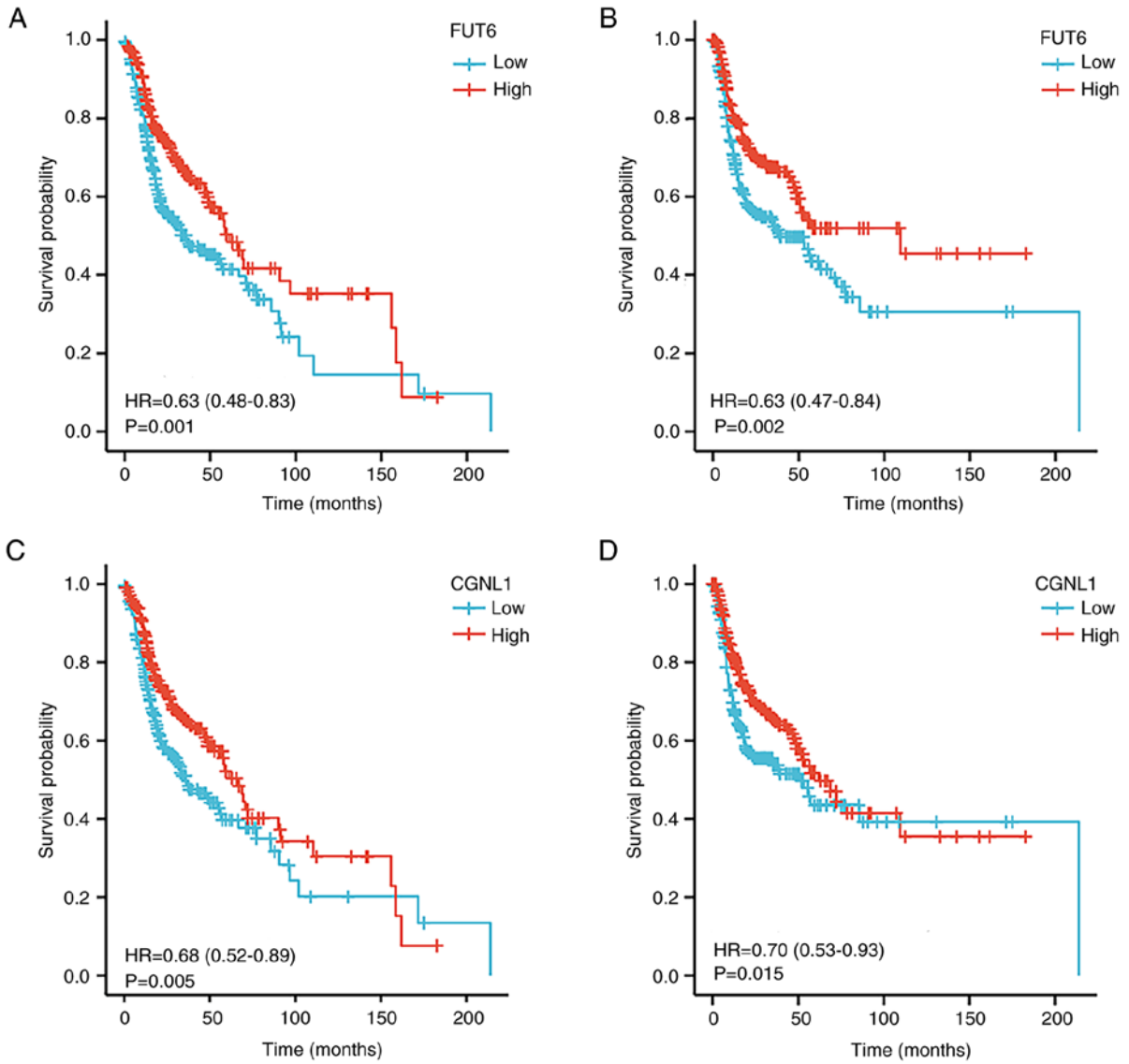

Figure 8. Survival analysis of FUT6 and CGNL1. (A) OS and (B) PFI curve of FUT6 differential expression in HNSCC. (C) OS and (D) PFI curve of CGNL1 differential expression in HNSCC. CGNL1, cingulin-like 1; FUT6, fucosyltransferase 6; OS, overall survival; HNSCC, head and neck squamous cell carcinoma; PFI, progression-free interval.

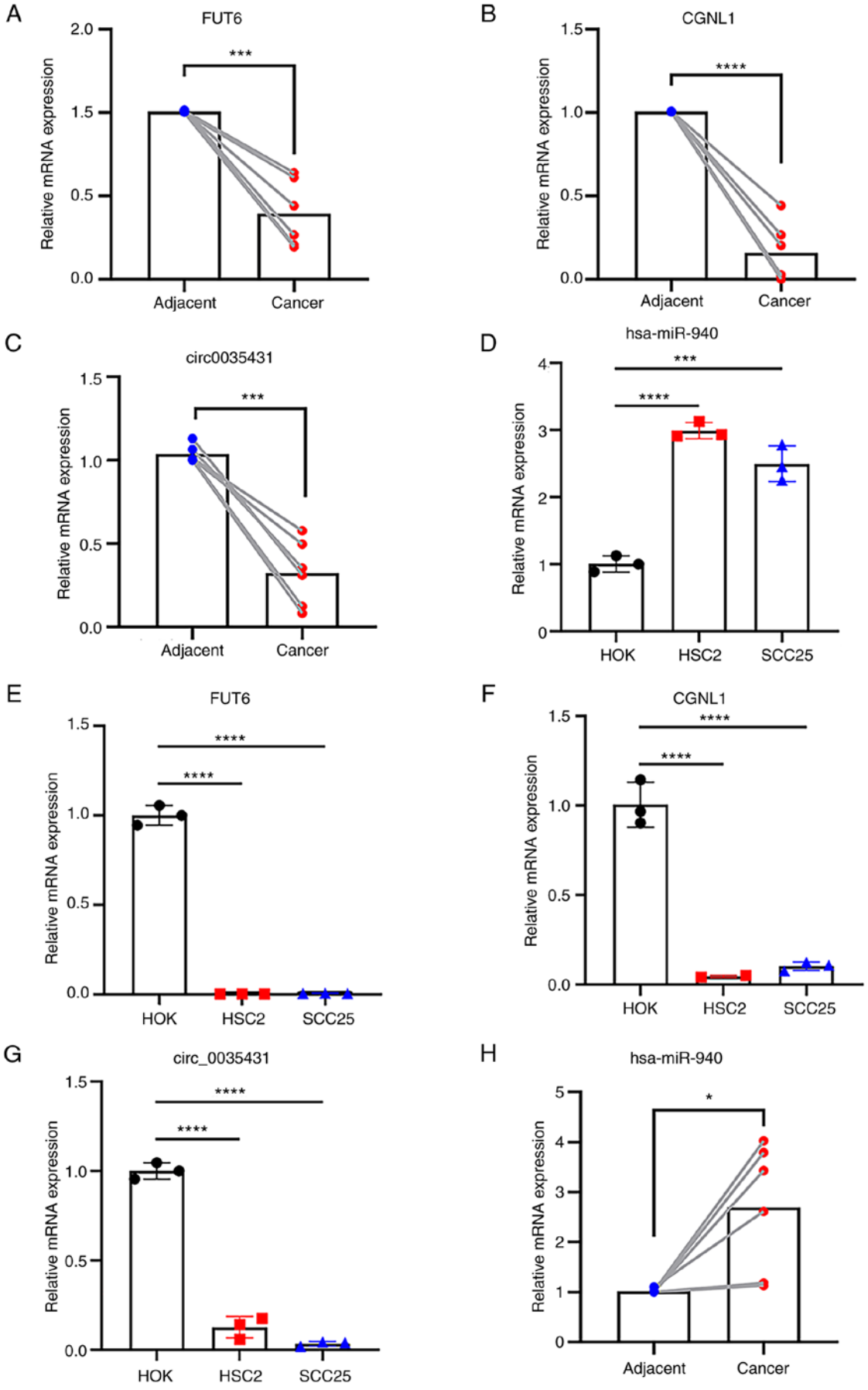

Figure 9. Reverse transcription-quantitative PCR validation of expression levels of hsa_circ_0035431, hsa-miR-940, FUT6 and CGNL1 in HNSCC tissues and cells. Transcription levels of (A) FUT6, (B) CGNL1, (C) hsa_circ_0035431 and (D) hsa_miR-940 in tissue. Transcription levels of (E) FUT6, (F) CGNL1, (G) hsa_circ_003543 and (H) hsa_miR-940 in HNSCC cell lines. *P<0.05, ***P<0.001, ****P<0.0001. FUT6, fucosyltransferase 6; CGNL1, cingulin-like 1; HNSCC, head and neck squamous cell carcinoma; circ, circular; miR, microRNA.

Table VII. Logistic regression analysis of cingulin-like 1.

Characteristic	n	Odds ratio (95% CI)	P-value
T2 vs. T1	177	0.720 (0.315-1.570)	0.419
T3 vs. T1	164	0.436 (0.190-0.953)	0.042[a]
T4 vs. T1	212	0.386 (0.171-0.828)	0.017[a]
N1 vs. N0	319	0.721 (0.430-1.198)	0.209
N2 vs. N0	393	1.170 (0.780-1.759)	0.448
N3 vs. N0	246	1.300 (0.281-6.718)	0.735
M1 vs. M0	477	0.244 (0.012-1.662)	0.208
Stage II vs. I	114	0.535 (0.175-1.475)	0.242
Stage III vs. I	121	0.379 (0.125-1.039)	0.068
Stage IV vs. I	291	0.462 (0.158-1.204)	0.128
Male vs. female	502	1.085 (0.730-1.613)	0.687
Age >60 vs. ≤60 years	501	0.901 (0.634-1.279)	0.561

[a]P<0.05.

RT-qPCR was performed to validate the accuracy of the microarray. miRNA-940 was highly expressed in HNSCC and FUT6 and CGNL1 were expressed at low levels. These results supported the hypothesis that hsa_circ_0035431 may act as a potential prognostic marker targeting and regulating the expression of FUT6 and CGNL1 through hsa-miR-940, thus affecting HNSCC progression.

However, the present study had numerous limitations. First, only six pairs of tumor tissue samples were used to validate circRNA/miRNA/mRNA interaction. Expression levels were only verified at the genetic level and further investigations into protein expression levels are required. In addition, western blot, immunohistochemistry, transfection, Transwell and wound healing assay and *in vivo* experiments are further required to validate the dysregulation of circRNA/miRNA/mRNA expression in HNSCC. Moreover, human papillomavirus infection status was not considered in the present study and may impact the progression and prognosis of HNSCC (48).

In conclusion, bioinformatics analysis revealed the potential regulatory mechanisms of the hsa_circ_0035431/hsa-miR-940/FUT6 and hsa_circ_0035431/hsa-miR-940/CGNL1 axes in development and prognosis of HNSCC. Notably, hsa_circ_0035431 may regulate expression of FUT6 and CGNL1 via sponging hsa-miR-940, thus impacting the progression and prognosis of HNSCC, and may exhibit potential as a drug target for the treatment of HNSCC.

Acknowledgements

Not applicable.

Funding

The present study was supported by National Natural Science Foundation of China (grant nos. 31900441 and 81903102), Natural Science Foundation of Shandong Province (grant nos. ZR2018BH026 and ZR2019PH075), Projects of Medical and Health Technology Development Program in Shandong Province (grant nos. 2017WS231 and 202008020682), Youth Project of Traditional Chinese Medicine Science and Technology in Shandong Province (grant no. 2020Q062) and Qilu Outstanding Young Talents in Health Project, Taishan Scholarship and Double-Hundred Foreign Talent Plan (grant no. WSG2018019).

Availability of data and materials

The datasets generated and/or analyzed during the current study are available in the Gene Expression Omnibus repository (accession no. GSE190224).

Authors' contributions

XYL and LLZ confirm the authenticity of all the raw data. XRM conceived the project. XYL, LLZ, and WLW designed the experiments and analyzed data. XYL and LLZ performed experiments. WLW, ZPL, FW, YW and SYZ were responsible for the collection of clinical samples and data. JD and XRM performed bioinformatics. XYL, LLZ and ZPL wrote the manuscript. All authors have read and approved the final manuscript.

Ethics approval and consent to participate

The experimental procedures were approved by The Ethics Committee of Binzhou Medical University Hospital (Binzhou, China; approval no. 2018-G010-01) and The West China Hospital of Stomatology, Sichuan University (Chengdu, China; approval no. WCHSIRB-CT-2021-022). All patients provided written informed consent.

Patient consent for publication

Not applicable.

Authors' information

LX, ORCID ID: 0000-0002-7288-7531. ZL, ORCID ID: 0000-0002-4454-4929. WW, ORCID ID: 0000-0001-7014-2985.

Competing interests

The authors declare that they have no competing interests.

References

1. Chow L: Head and neck cancer. N Engl J Med 382: 60-72, 2020.
2. Wang J, Chen X, Tian Y, Zhu G, Qin Y, Chen X, Pi L, Wei M, Liu G, Li Z, *et al*: Six-gene signature for predicting survival in patients with head and neck squamous cell carcinoma. Aging (Albany NY) 12: 767-783, 2020.
3. Garbo S, Maione R, Tripodi M and Battistelli C: Next RNA therapeutics: The mine of Non-coding. Int J Mol Sci 23: 7471, 2022.
4. Tang X, Ren H, Guo M, Qian J, Yang Y and Gu C: Review on circular RNAs and new insights into their roles in cancer. Comput Struct Biotechnol J 19: 910-928, 2021.
5. Qiu S, Li B, Xia Y, Xuan Z, Li Z, Xie L, Gu C, Lv J, Lu C, Jiang T, *et al*: CircTHBS1 drives gastric cancer progression by increasing INHBA mRNA expression and stability in a ceRNA- and RBP-dependent manner. Cell Death Dis 13: 266, 2022.
6. Yang J, Qi M, Fei X, Wang X and Wang K: Hsa_circRNA_0088036 acts as a ceRNA to promote bladder cancer progression by sponging miR-140-3p. Cell Death Dis 13: 322, 2022.
7. Mo M, Liu B, Luo Y, Tan J, Zeng X, Zeng X, Huang D, Li C, Liu S and Qiu X: Construction and comprehensive analysis of a circRNA-miRNA-mRNA regulatory network to reveal the pathogenesis of hepatocellular carcinoma. Front Mol Biosci 9: 801478, 2022.
8. Nath M, Roy D and Choudhury Y: Circular RNAs are potential prognostic markers of head and neck squamous cell carcinoma: Findings of a Meta-analysis study. Front Oncol 12: 782439, 2022.
9. Wu Y, Zhang Y, Zheng X, Dai F, Lu Y, Dai L, Niu M, Guo H, Li W, Xue X, *et al*: Circular RNA circCORO1C promotes laryngeal squamous cell carcinoma progression by modulating the let-7c-5p/PBX3 axis. Mol Cancer 19: 99, 2020.
10. Kim D, Langmead B and Salzberg SL: HISAT: A fast spliced aligner with low memory requirements. Nat Methods 12: 357-360, 2015.
11. Robinson MD, Mccarthy DJ and Smyth GK: edgeR: A Bioconductor package for differential expression analysis of digital gene expression data. Bioinformatics 26: 139-140, 2010.
12. Young MD, Wakefield MJ, Smyth GK and Oshlack A: Gene ontology analysis for RNA-seq: Accounting for selection bias. Genome Biol 11: R14, 2010.
13. Ke MJ, Ji LD and Li YX: Explore prognostic marker of colorectal cancer based on ceRNA network. J Cell Biochem 120: 19358-19370, 2019.
14. Enright AJ, John B, Gaul U, Tuschl T, Sander C and Marks DS: MicroRNA targets in drosophila. Genome Biol 5: R1, 2003.
15. Kruger J and Rehmsmeier M: RNAhybrid: microRNA target prediction easy, fast and flexible. Nucleic Acids Res 34: W451-W454, 2006.
16. Knapek KJ, Georges HM, Van Campen H, Bishop JV, Bielefeldt-Ohmann H, Smirnova NP and Hansen TR: Fetal lymphoid organ immune responses to transient and persistent infection with bovine viral diarrhea virus. Viruses 12: 816, 2020.
17. Garcia-Hidalgo MC, Gonzalez J, Benitez ID, Carmona P, Santisteve S, Perez-Pons M, Moncusi-Moix A, Gort-Paniello C, Rodriguez-Jara F, Molinero M, *et al*: Identification of circulating microRNA profiles associated with pulmonary function and radiologic features in survivors of SARS-CoV-2-induced ARDS. Emerg Microbes Infect 11: 1537-1549, 2022.
18. Djebali S, Davis CA, Merkel A, Dobin A, Lassmann T, Mortazavi A, Tanzer A, Lagarde J, Lin W, Schlesinger F, *et al*: Landscape of transcription in human cells. Nature 489: 101-108, 2012.
19. Zhang Z, Zhang J, Diao L and Han L: Small non-coding RNAs in human cancer: Function, clinical utility, and characterization. Oncogene 40: 1570-1577, 2021.
20. Yousefi H, Maheronnaghsh M, Molaei F, Mashouri L, Reza AA, Momeny M and Alahari SK: Long noncoding RNAs and exosomal lncRNAs: Classification, and mechanisms in breast cancer metastasis and drug resistance. Oncogene 39: 953-974, 2020.
21. Guo L, Jia L, Luo L, Xu X, Xiang Y, Ren Y, Ren D, Shen L and Liang T: Critical roles of circular RNA in tumor metastasis via acting as a sponge of miRNA/isomiR. Int J Mol Sci 23: 7024, 2022.
22. Prats AC, David F, Diallo LH, Roussel E, Tatin F, Garmy-Susini B and Lacazette E: Circular RNA, the key for translation. Int J Mol Sci 21: 8591, 2020.
23. Zhou R, Wu Y, Wang W, Su W, Liu Y, Wang Y, Fan C, Li X, Li G, Li Y, *et al*: CircularRNAs (circRNAs) incancer. Cancer Lett 425: 134-142, 2018.
24. Derks KW, Misovic B, van den Hout MC, Kockx CE, Gomez CP, Brouwer RW, Vrieling H, Hoeijmakers JH, van Ijcken WF and Pothof J: Deciphering the RNA landscape by RNAome sequencing. RNA Biol 12: 30-42, 2015.
25. Szabo L and Salzman J: Detecting circular RNAs: Bioinformatic and experimental challenges. Nat Rev Genet 17: 679-692, 2016.
26. Zheng R, Zhang K, Tan S, Gao F, Zhang Y, Xu W, Wang H, Gu D, Zhu L, Li S, *et al*: Exosomal circLPAR1 functions in colorectal cancer diagnosis and tumorigenesis through suppressing BRD4 via METTL3-eIF3h interaction. Mol Cancer 21: 49, 2022.
27. Wang Z, Sun A, Yan A, Yao J, Huang H, Gao Z, Han T, Gu J, Li N, Wu H and Li K: Circular RNA MTCL1 promotes advanced laryngeal squamous cell carcinoma progression by inhibiting C1QBP ubiquitin degradation and mediating beta-catenin activation. Mol Cancer 21: 92, 2022.
28. Gao F, Han J, Wang Y, Jia L, Luo W and Zeng Y: Circ_0109291 promotes cisplatin resistance of oral squamous cell carcinoma by sponging miR-188-3p to increase ABCB1 expression. Cancer Biother Radiopharm 37: 233-245, 2022.
29. Qi X, Zhang DH, Wu N, Xiao JH, Wang X and Ma W: ceRNA in cancer: Possible functions and clinical implications. J Med Genet 52: 710-718, 2015.
30. Thomson DW and Dinger ME: Endogenous microRNA sponges: Evidence and controversy. Nat Rev Genet 17: 272-283, 2016.
31. Ge P, Chen X, Liu J, Jing R, Zhang X and Li H: Hsa_circ_0088036 promotes nonsmall cell lung cancer progression by regulating miR-1343-3p/Bcl-3 axis through TGFβ/Smad3/EMT signaling. Mol Carcinog 62: 1073-1085, 2023.
32. Shen Y, Zhang N, Chai J, Wang T, Ma C, Han L and Yang M: CircPDIA4 induces gastric cancer progressionby promoting ERK1/2 activation and enhancing biogenesisof oncogenic circRNAs. Cancer Res 83: 538-552, 2023.
33. Mo H, Shen J, Zhong Y, Chen Z, Wu T, Lv Y, Xie Y and Hao Y: CircMAN1A2 promotes vasculogenic mimicry of nasopharyngeal carcinoma cells through upregulating ERBB2 via sponging miR-940. Oncol Res 30: 187-199, 2022.
34. Dang Y, Ouyang X, Zhang F, Wang K, Lin Y, Sun B, Wang Y, Wang L and Huang Q: Circular RNAs expression profiles in human gastric cancer. Sci Rep 7: 9060, 2017.
35. Fan Y, Che X, Hou K, Zhang M, Wen T, Qu X and Liu Y: MiR-940 promotes the proliferation and migration of gastric cancer cells through up-regulation of programmed death ligand-1 expression. Exp Cell Res 373: 180-187, 2018.
36. Liu X, Ge X, Zhang Z, Zhang X, Chang J, Wu Z, Tang W, Gan L, Sun M and Li J: MicroRNA-940 promotes tumor cell invasion and metastasis by downregulating ZNF24 in gastric cancer. Oncotarget 6: 25418-25428, 2015.
37. Su K, Wang C, Zhang Y, Cai Y, Zhang Y and Zhao Q: miR-940 upregulation contributes to human cervical cancer progression through p27 and PTEN inhibition. Int J Oncol 50: 1211-1220, 2017.
38. Cheng L, Luo S, Jin C, Ma H, Zhou H and Jia L: FUT family mediates the multidrug resistance of human hepatocellular carcinoma via the PI3K/Akt signaling pathway. Cell Death Dis 4: e923, 2013.
39. Dai Y, Cheng Z, Pang Y, Jiao Y, Qian T, Quan L, Cui L, Liu Y, Si C, Chen J, *et al*: Prognostic value of the FUT family in acute myeloid leukemia. Cancer Gene Ther 27: 70-80, 2020.
40. Mai Z, Chen H, Huang M, Zhao X and Cui L: A robust metabolic enzyme-based prognostic signature for head and neck squamous cell carcinoma. Front Oncol 11: 770241, 2022.
41. Wei X, Luo T, Li J, Xue Z, Wang Y, Zhang Y, Chen Y and Peng C: Development and validation of a prognostic classifier based on lipid metabolism-related genes in gastric cancer. Front Mol Biosci 8: 691143, 2021.

42. Li N, Liu Y, Miao Y, Zhao L, Zhou H and Jia L: MicroRNA-106b targets FUT6 to promote cell migration, invasion, and proliferation in human breast cancer. IUBMB Life 68: 764-775, 2016.
43. Chrifi I, Hermkens D, Brandt MM, van Dijk C, Burgisser PE, Haasdijk R, Pei J, van de Kamp E, Zhu C, Blonden L, *et al*: Cgnl1, an endothelial junction complex protein, regulates GTPase mediated angiogenesis. Cardiovasc Res 113: 1776-1788, 2017.
44. Lu X, Jing L, Liu S, Wang H and Chen B: miR-149-3p is a potential prognosis biomarker and correlated with immune infiltrates in uterine corpus endometrial carcinoma. Int J Endocrinol 2022: 5006123, 2022.
45. Li W, Wang S, Qiu C, Liu Z, Zhou Q, Kong D, Ma X and Jiang J: Comprehensive bioinformatics analysis of acquired progesterone resistance in endometrial cancer cell line. J Transl Med 17: 58, 2019.
46. Jin Y and Qin X: Significance of TP53 mutation in treatment and prognosis in head and neck squamous cell carcinoma. Biomark Med 15: 15-28, 2021.
47. Song Y, Jin D, Ou N, Luo Z, Chen G, Chen J, Yang Y and Liu X: Gene expression profiles identified novel urine biomarkers for diagnosis and prognosis of high-grade bladder urothelial carcinoma. Front Oncol 10: 394, 2020.
48. Kutz LM, Abel J, Schweizer D, Tribius S, Krull A, Petersen C and Loser A: Quality of life, HPV-status and phase angle predict survival in head and neck cancer patients under (chemo)radiotherapy undergoing nutritional intervention: Results from the prospective randomized HEADNUT-trial. Radiother Oncol 166: 145-153, 2022.